EARTHQUAKE ENGINEERING AND STRUCTURAL DYNAMICS, VOL. 27, 1–14 (1998)

# ANALYTICAL AND CENTRIFUGE STUDIES OF PILE GROUPS IN LIQUEFIABLE SOIL BEFORE AND AFTER SITE REMEDIATION

A. OHTSUKI*†, K. FUKUTAKE‡ AND M. SATO‡

*Institute of Technology, Shimizu Corporation, 4-17, Etchujima 3-chome, Koto-ku, Tokyo 135, Japan*

## SUMMARY

The objectives of this paper are to show practically: (1) the validation of a proposed three-dimensional effective stress analysis for the pile foundations, and (2) the effectiveness of remedial deposits on pile stresses under liquefaction by making comparisons between the results of centrifuge tests and those of the proposed analysis. Two foundation models supported by end-bending piles were studied with improved and unimproved deposits.

There exists a good consistency between the numerical and experimental results for excess pore water-pressure ratios ranging from 0 to about 0·9. From the numerical results, the bending moment at the pile top with the improved deposit is about 50 per cent lower than that with the unimproved deposit. However, it was found that the smaller the bending moment develops in the pile with the improved deposit, the larger the compressive and/or tensional axial stresses in the pile. This is due to the predominant excitation of rocking vibration of the foundation.

From the analytical and experimental results, it has been found that the remedial method can be a variable means to protect piles from soil liquefaction hazards. However, both axial stress and bending moment produced in piles should be considered in assessing the liquefied seismic capacity of group pile-foundation–structural systems with improved soil deposits. © 1998 John Wiley & Sons, Ltd.

*Earthquake Engng. Struct. Dyn.*, **27**, 1–14 (1998)

KEY WORDS: liquefaction; ground-improvement method; pile groups in liquefiable soil; centrifuge dynamic test; three-dimensional effective-stress method

## INTRODUCTION

Liquefaction and post-liquefaction occurred in widespread areas along the shoreline and reclaimed islands in Kobe, Japan, during the Hyogo-ken Nambu earthquake on 17th January 1995, known as the Kobe earthquake (Japan Society of Civil Engineers, 1995). There were extensive damages to structures and pile foundations caused by the liquefaction and/or the large lateral displacements of the ground. Important structures, such as high-rise buildings, bridges, oil tanks, industrial complex facilities and dikes are supported by piles to prevent seismic damage. In some areas, both the piles and the improved deposit have been used together. Although the behaviour of piles in liquefied deposits have been studied by many researchers, the effects of remedial deposits on pile stresses have not been clarified.

The authors developed a three-dimensional effective-stress method to evaluate the response of the pile–structure system standing on liquefiable ground. To examine the effectiveness of remedial measures as a means to protect group-pile foundations from liquefaction hazard, we compared the response of foundations supported by piles and improved soil on the perimeter of the piles foundation. The results obtained by

* Correspondence to: A. Ohtsuki, Shimizu Corporation, Institute of Technology, 4-17, Etchujima, 3-chome, Koto-ku, Tokyo 135, Japan. E-mail: ohts@sit.shimz.co-jp

† Chief Researcher

‡ Senior Researcher

CCC 0098–8847/98/010001–14$17·50



*Received 3 July 1996*

*Revised 18 March 1997*

the new three-dimensional method and the centrifuge shaking test suggest that this methodology is applicable for pile–structures standing on liquefiable ground.

## OUTLINE OF NUMERICAL METHOD

Several studies have been conducted on the non-linear response of piles based on the Winkler model. The beam-on-Winkler foundation was introduced by Nogami *et al.*[1] They proposed originally the Kelvin model with a consistent mass. Trochnis[2] utilized a model of viscoplasticity to describe the non-linear springs between soil and piles. Badoni and Makris[3] have recently proposed hysteresis springs and frequency-dependent dashpot. In those studies, the response of piles in liquefiable deposit was not examined.

Tazoh and Shimizu[4] examined the effective seismic motion and the pile head impedance for the non-linear behaviour of deposits by making a comparison between the results of a shaking table test and analyses. Kagawa and Kraft[5] formulated and examined the lateral-pile response during liquefaction using the beam-on-Winkler foundation model, which accounts for the non-linear interaction springs arising between the ground and piles. Tokimatsu and Nomura[6] and Miyamoto *et al.*[7] succeeded in simulating the response of a pile–structure system by using a similar model.

These simplified methods are useful to counteract the non-linear soil–pile interaction. They can represent the response of a foundation to strong vibrations approximately. However, it is difficult for the methods to properly assess the horizontal and rocking spring constants between the piles and the surrounding improved soil, which exist on the perimeter of the pile-foundation system, because these spring constants depend on the accumulation of the excess pore water-pressure. Although these models can simulate the response of superstructures, the axial stress of the pile at different depths cannot be estimated directly from the rocking spring; other models, for instance FEM, would be needed.

FEM can avoid the problems by associating well a beam-on-Winkler foundation model. Zienkiewicz and Shiomi[8] and Prevost[9] developed methods to solve the two-phase equation proposed by Biot[10] for two-dimensional liquefaction problems. The two-phase equation has the advantage of expressing the dissipation of excess pore water-pressure and evaluating the settlement of deposits. The method, however, requires a significantly large amount of computation and memory capacity, and has been applied only in a very crude manner.

In contrast, the two-dimensional effective-stress methods, assuming the undrained condition and the movement of water and soil together, can reduce the computing-time and memory-capacity requirements considerably compared to the method based on the two-phase equation. They were proposed by Finn *et al.*[11,12] and Ohtsuki *et al.*[13–15] The characteristics of the methods are to solve the governing equation for soil with bulk modulus of water for the excess pore water-pressure.

For three-dimensional problems, we initially proposed the effective-stress method with a new soil model. In a previous published paper,[16] the authors showed that the proposed method can simulate well the results of shaking table tests of saturated soil–piles–structure-system, and examined the behaviour of piles in unimproved ground under the gravity of 1 g.

The method can be applied to a real problem with many degrees of freedom. The method is highly effective in computing three-dimensional problems, because (1) the equation of motion was solved explicitly, (2) the space region was formulated by the finite element method with one Gaussian integration point, and Hallquist method [17] was used to surpass hourglass modes and (3) a simplified constitutive model was used.

### *Outline of constitutive equation*

A complicated constitutive equation may represent the actual phenomenon accurately, but it tends to involve complex formulation with many parameters and needs a considerable amount of memory capacity in a computer. Hence, a simplified constitutive model was used to represent the non-linear behaviour of the soil

 

under liquefaction. The proposed constitutive model involves a stress–strain and a strain–dilatancy relationships as follows:

(1) The modified Ramberg–Osgood model, which was proposed by Tatuoka and Fukushima[18] and is suitable for expressing the simple shear stress and strain condition, was extended to three-dimensional problems.

(2) To calculate the dilatancy from the shear strain, a bowl model proposed by Fukutake and Matsuoka[19,20]. Fukutake and Ohtsuki[21] was used as a three-dimensional dilatancy model. The bowl model, which is based on multi-directional simple shearing strains, enables to calculate the amount of dilatancy from shear strains under the random path. Figure 1 shows the relationship of the Ramberg–Osgood model and the bowl model.

This model, which concentrates on the performance of shear stress and strain, can represent the response of a soil–structure system well in layered ground, where the horizontal shearing deformation predominates during a large earthquake. The model does not apply well to cases where the normal strains are predominant.

## EXPERIMENTAL MODELLING

Geotechnical centrifuge tests have proven to be very effective means for investigating problems in soil mechanics under prototype stress conditions proposed by Schofild,[22] Scott,[23] Prevost and Scanlan[24] and others. Sato,[25,26] the third author, also developed a centrifuge simulator to assess the soil–structure interaction. The arm radius of the centrifuge to the basket platform is 3·31 m for dynamic tests. An electromagnetic shaking table of 950 mm length and 450 mm width was put on the centrifuge simulator.

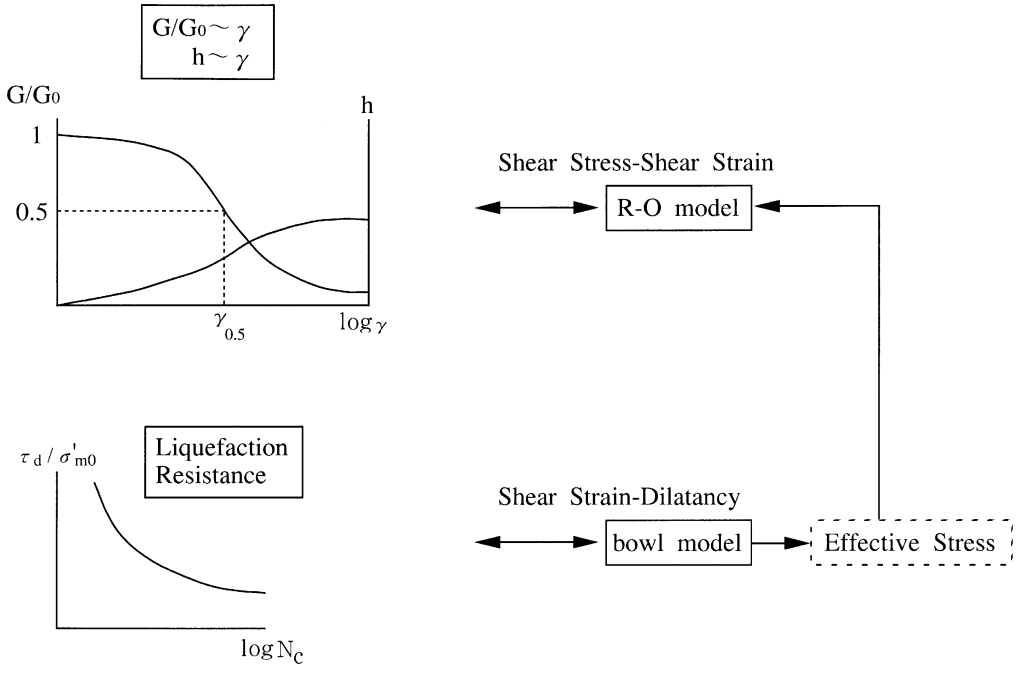


Figure 1. Relationship between R–O and bowl models

 

Figure 2 shows a laminar container on the shaking table with inside dimensions of 300 mm height, 770 mm length and 475 mm width. The container consisted of rectangular hollow frames made of square steel tubes. Linear bearings were installed between these frames to reduce friction during shaking.

Toyoura sand was used with a relative density of about 60 per cent for the surface layer. Gravel was used in the bottom layer. Silicon oil of high viscosity, 30 times as viscous as water, was used in place of water to satisfy the similitude requirements. The silicon level was maintained at the surface of the deposit.

As shown in Figure 2, the superstructure has a mass of 12·4 kg and the foundation has a mass of 6 kg, both made of layered steel plates. The pillar was made of four rectangular steel plates of height 100 mm, length 12 mm and width 5 mm. A dashpot made of asphalt gum was attached between the superstructure and the foundation to provide structural damping during shaking. The natural frequency and damping ratio of the structure were about 50 Hz and 5 per cent, respectively. The superstructure was idealized by a single-degree-of-freedom system. Four piles were fixed at the foundation slab. The piles were of diameter 10 mm, thickness 1 mm and were made of aluminum. The bending stiffness of the pile was $2{\cdot}14 \times 10^{-4}$ kgf/cm$^2$ ($2{\cdot}01 \times 10^{-3}$ MPs). All the pile tips were inserted into the bearing stratum of gravel and their horizontal movements were fixed.

Figure 2 also shows the accelerometers, indicated by circles, in the deposit (A1, A2), and attached to the structure (A3). The pore pressure transducers, shown by squares, were placed in natural ground (P1–P3). The

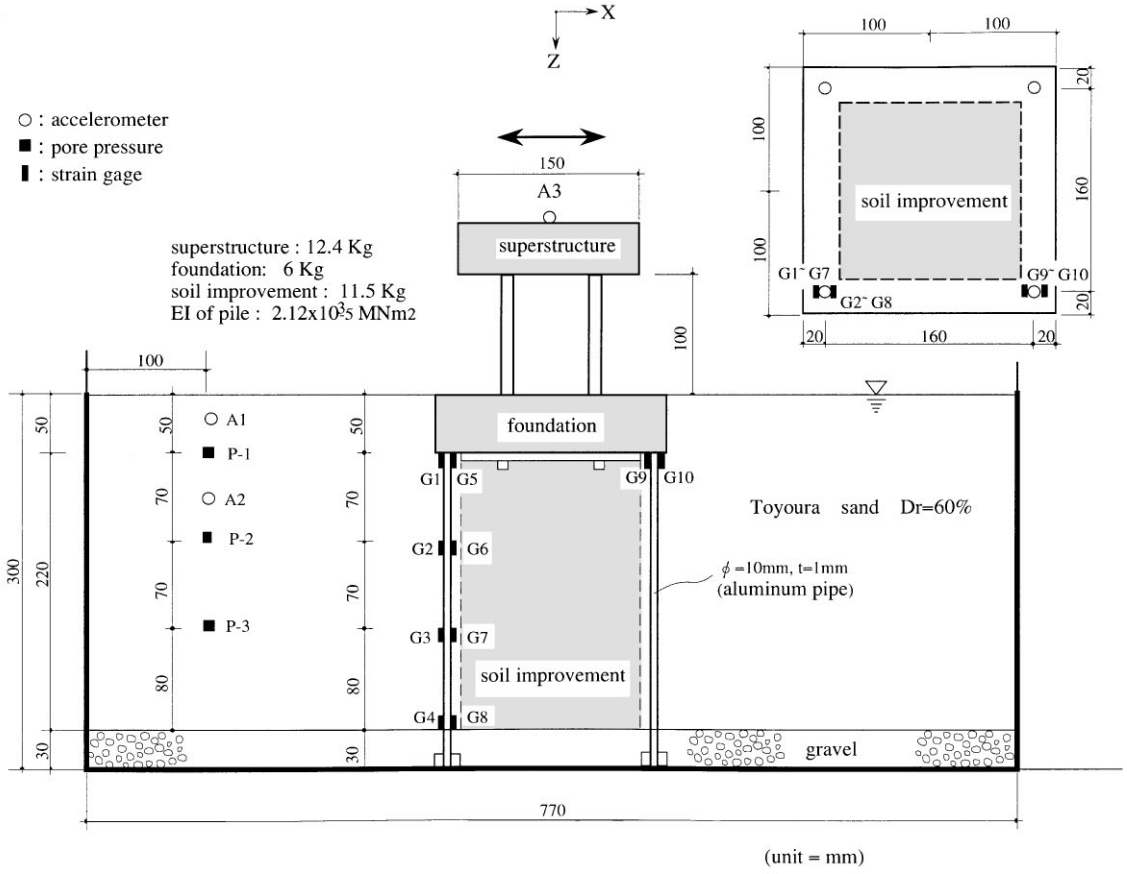


Figure 2. Experimental model (unit = mm)

 

strain gauges, shown by rectangles, were attached to the pile (G1–G10) to measure the bending and axial strains of the piles.

Two structural types were considered.

*Case* 1: End-bending piles in unimproved soil.
*Case* 2: End-bending piles in improved soil covering a 160 mm square area.

The pile group used in the test was composed of four piles and only the soil among these piles was improved. The improved area occupies 64 per cent of the base foundation area. The mass of soil improved which was made of soil cement was 11·5 kg and its shear modulus, uniform in the improved soil area, was 5000 kg/cm$^2$ ($4{\cdot}70 \times 10^2$ MPs) under a principal stress of 1 kg/cm$^2$.

The test was run in a field of 25 G using the Tokachi-oki earthquake record in E–W component of May 1968 with a maximum acceleration of about 5 G. A scale model to prototype was adopted as 1:25 and the similitude requirements used in the tests are listed in Table I.

## ANALYTICAL MODEL

The analytical model including the four piles in the liquefiable deposit was modelled by 3344 solid elements and 984 beam elements as indicated in Fig. 3. The top of the piles were fixed against rotation. Nodes at the base of the model were fixed against both vertical and horizontal movements. Nodes on the outer boundary were fixed against vertical movements. The pile is treated as volumeless and replaced by vertical beam elements in the present analysis. The beam elements were inserted among the solid elements, and consequently lift-up of the pile from the deposit was not considered. When the number of piles is few and the pile-to-pile distance is large, the effect of a volume of pile on the non-linear response of the system is considered to be small. To obtain the precise solution of the above problem, Nogami model[1] is one of the applicable methods.

Table I. The similitude requirements used in the test

| | | Scale ratio | Unit | Model | Prototype |
|---|---|---|---|---|---|
| Sand stratum | Thickness | $1/\lambda$ | m | 7·5 | 0·3 |
| | Density | 1 | g/cm$^3$ | 1·73 | 1·73 |
| | Permeability | $1/\lambda$ | cm/s | $2{\cdot}25 \times 10^{-2}$ | $9 \times 10^{-4}$ |
| Bearing stratum | Thickness | $1/\lambda$ | m | 0·75 | 0·03 |
| Pile | Length of pile | $1/\lambda$ | m | 6·25 | 0·25 |
| | Diameter | $1/\lambda$ | cm | 25 | 1 |
| | Thickness | $1/\lambda$ | mm | 25 | 1 |
| | Young's modulus | 1 | MN/m$^2$ | 73 000 | 73 000 |
| | Geometrical moment of inertia | $1/\lambda^4$ | cm$^4$ | 11 328 | 0·029 |
| | Bending stiffness | $1/\lambda^4$ | MN/m$^2$ | 8·28 | $2{\cdot}12 \times 10^{-5}$ |
| Footing | Mass | $1/\lambda^3$ | kg | 93 750 | 6 |
| | Length (depth) | $1/\lambda$ | m | 1·25 | 0·05 |
| Structure | Mass | $1/\lambda^3$ | kg | 334 800 | 12·4 |
| | Natural frequency | $\lambda$ | Hz | 2 | 50 |
| | Damping ratio | 1 | % | 5·0 | 5·0 |
| Exciting acceleration | | $\lambda$ | g | 0.2 | 5 |

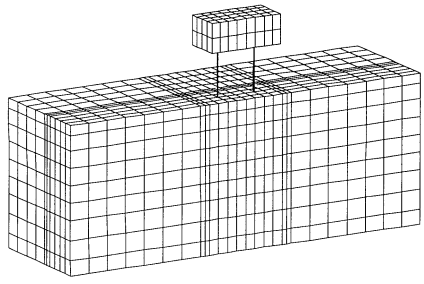

Figure 3. Three-dimensional-mesh model for a single-degree-of-freedom system supported by group piles in a saturated sandy deposit

Table II. Soil parameters used in the test

| | R–O model | | | Bowl model | | | | |
|---|---|---|---|---|---|---|---|---|
| | $Go_i$ | $\gamma_{0.5i}$ | $h_{max}$ | $A$ | $C$ | $D$ | $C_s/(1+e_0)$ | $X_e$ |
| Sand stratum | 1500 | 0·00019 | 0·27 | − 2·5 | 9·0 | 25 | 0·007 | 0·11 |
| Bearing stratum | 3130 | 0·00013 | 0·27 | − 7·0 | 40 | 60 | 0·005 | — |

$Go_i$ and $\gamma_{0.5i}$ are values under $\sigma'_m = 1$ ft/m$^2$ = 98 MPa
The symbols for the parameters of the soil model are shown in References 19–21

The soil parameters were estimated from previously available data on Toyoura sand with a relative density of 60 per cent. The parameters for the constitutive model are listed in Table II. The parameters of the R–O model are determined by cyclic triaxial tests. The values of the bowel model were obtained by fitting the liquefaction resistance curve.

## EXAMINATION OF THE RESPONSE OF SOIL–PILE SYSTEM

*Results of case 1*

Figure 4 illustrates the time histories of the computed and observed excess pore water-pressure ratios at P1–P3: the solid and broken lines correspond to the computed and observed results, respectively. In this paper, the excess pore water-pressure ratio is defined as $(\sigma'_{m0} - \sigma'_m)/\sigma'_{m0}$, where $\sigma'_{m0}$ is the initial effective mean-stress and $\sigma'_m$ the effective mean-stress during shaking.

Figure 4 shows that the accumulation of measured excess pore water-pressure at P1 was faster than that of the analytical model. The observed and computed excess pore water-pressure ratio at P1 appeared at about 0·99 and 0·8 at 0·15 s, respectively. It is found from the difference of 0·99 and 0·8, that the prototype deposit liquefied, while the analytical model did not. Comparing the observed and computed results of P2 and P3, we found that both results agreed well in the amplitudes and the starting time of accumulation of the excess pore water-pressure ratio.

Figure 5 shows the time histories of the computed and observed accelerations in the soil deposit: the solid and broken lines correspond to the computed and observed results, respectively. The computed and observed accelerations indicate that the two results agreed well with each other in amplitudes and vibration phases. The maximum acceleration measured was 100 m/s$^2$ whereas the computed value was 50 m/s$^2$ around 0·25 s in A2. It was found that both the measured and computed accelerations in A1 and A2 were reduced to smaller values and longer periods prevailed, which indicates a typical property of acceleration under liquefaction after a time of about 0·2 or 0·3 s in A1 and in A2, respectively.

 

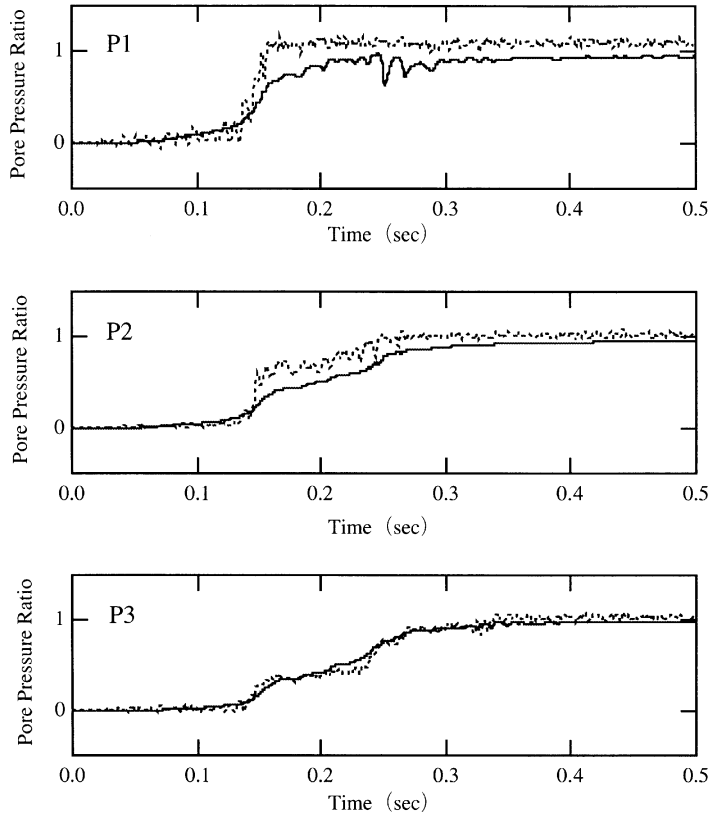


Figure 4. Computed and observed excess pore water presure ratios at P1, P2 and P3 for case 1 (—— computed ----- observed)

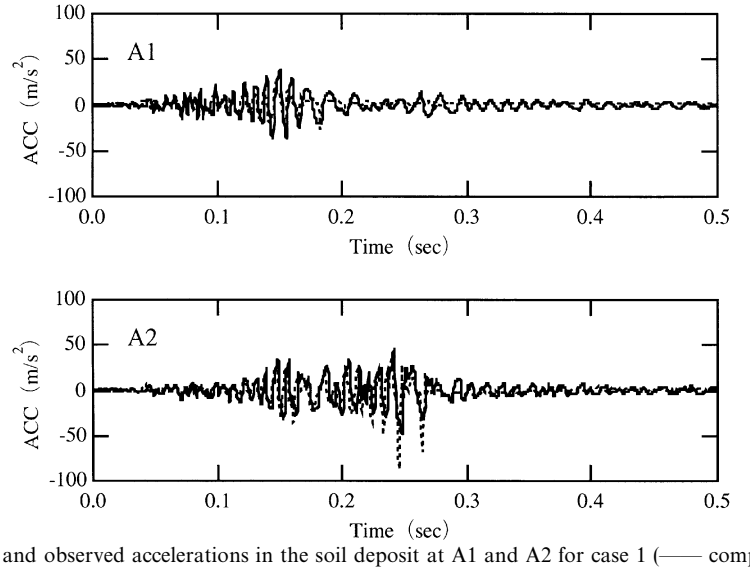


Figure 5. Computed and observed accelerations in the soil deposit at A1 and A2 for case 1 (—— computed, ----- observed)

 

Figure 6 shows time histories of the observed and computed accelerations of the structure at A3 and the bending moment of the pile at G1. For the acceleration at the top of structure at A3, a relatively good agreement existed between the numerical and experimental results from the start of shaking till 0·15 s. However, both results differed, after the liquefaction which occurred at P1 around 0·15 s. The computed amplitude of A3 is about 0·5 times that of the measured one. This is the reason why the computed horizontal soil stiffness around the pile was larger than that for the real deposit under liquefaction.

The observed bending moments were converted from the measured bending strains of the aluminum pile. It is shown in Figure 6 that the computed and observed vibration phases generally agree well at G1, for time periods less than 0·3 s. From 0·25 to 0·5 s, the computed moment drifted. The relationship between shear stress and shear strain is shown in Figure 7. It indicates that the residual shear strain occurred around P1 which may be the cause for the drifting of the component of the bending moment at G1 after a time of 0·35 s.

*Results of case 2*

Figures 8 and 9 show the pore water-pressure ratio and the ground acceleration for case 2. The figures show that the observed and computed vibration phases at P1–P3, and A1 and A2 agreed well, although the agreement in amplitude was poorer at shallower locations, A1 and P1. During liquefaction, a value of 1·0 of the pore water-pressure ratio, occurred approximately around 0·2 s in the observed data. The computed pore water-pressure ratio had a value of 0·7. For the computed pore water-pressure ratios ranging from 0·7 to 0·9, the soil stiffness does not reduce noticeably, so that the computed acceleration was larger than the observed one from 0·2 to 0·35 s. Figure 10 shows the acceleration at the top of the structure A3. The computed and observed vibration phases of the acceleration agree relatively well within the first 0·3 s. However, the amplitude of measured acceleration was larger than that of the computed one after 0·3 s. This is due to the

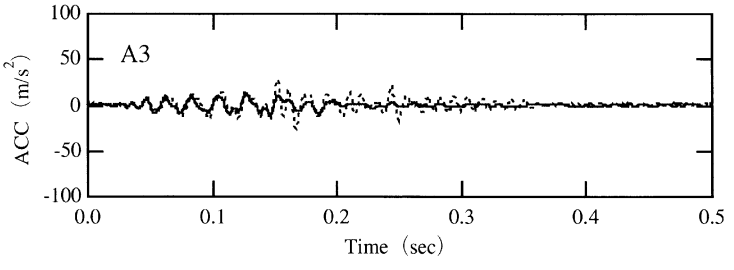


acceleration of the structure

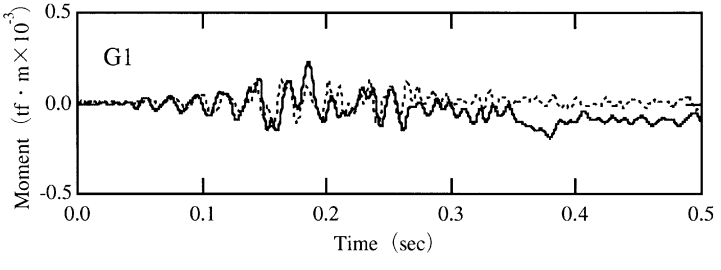


bending moment of the pile

Figure 6. Computed and observed accelerations of the structure at A3, and bending moment of the pile at G1 for case 1 (—— computed, ----- observed)

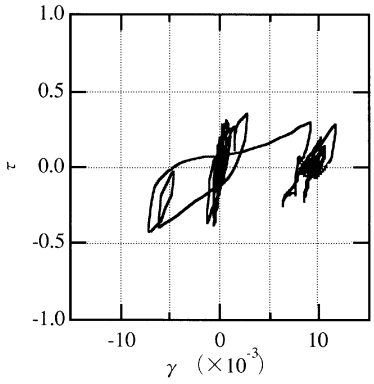


Figure 7. Relationship between shear stress (tf/m$^2$) and shear strain at P1 for case 1

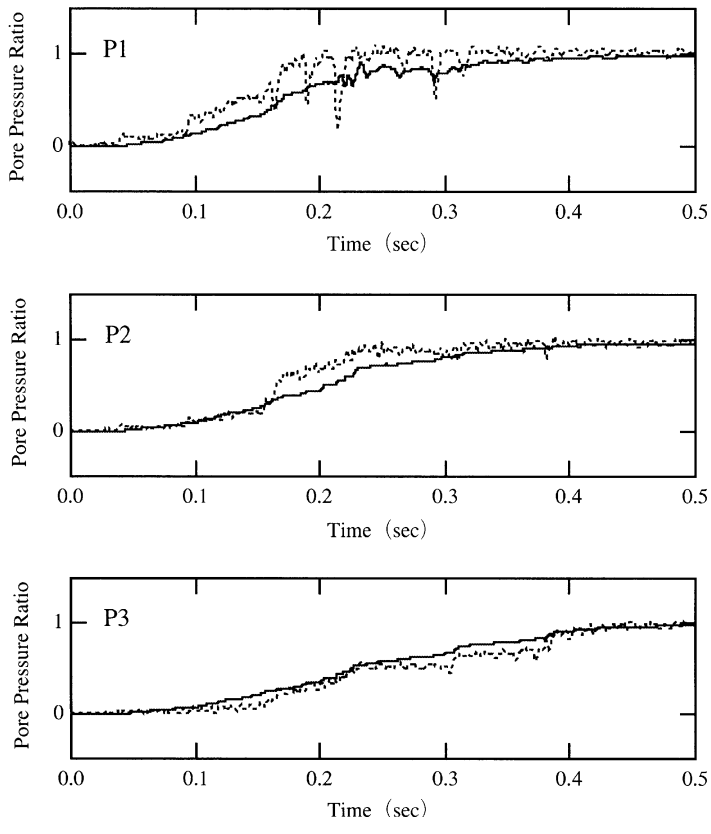


Figure 8. Computed and observed excess pore water-pressure ratios at P1, P2 and P3 for case 2 (—— computed, ----- observed)

following: (1) the horizontal springs between soil and piles for the analytical model were much stiffer than that of the prototype model after 0·3 s, so that the observed response of the structure is considered to be larger than that of the computed one, and (2) the damping of the prototype superstructure was different from that used in the analysis.

 

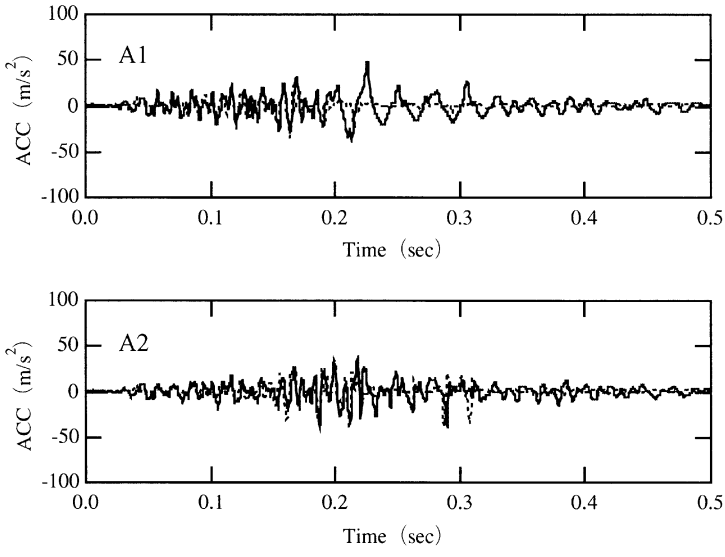


Figure 9. Computed and observed accelerations in the soil deposit at A1 and A2 for case 2 (—— computed, ----- observed)

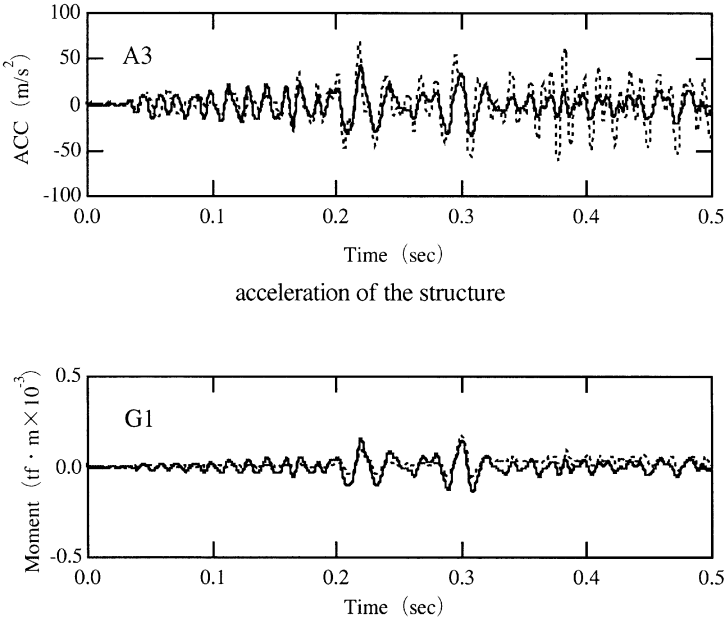


Figure 10. (top) Computed and observed accelerations of the structure at A3 and (bottom) bending moment of the pile at G1 for case 2 (—— computed, ----- observed)

Comparing the acceleration time histories for cases 1 and 2, it was noticed that the amplitudes of the measured and computed accelerations at A3 for case 2 were larger than those for case 1. There are two reasons for this: (1) the superstructure on unimproved soil was isolated from the vibration by the liquefied soil deposit, and (2) the superstructure on improved soil was vibrated by the wave motion transferred

 

through the improved soil whose shear modulus was 5000 kgf/cm$^2$ ($4{\cdot}70 \times 10^2$ MPa) and damping was smaller even when the surrounding soil was liquefied.

Figure 10 also shows the time histories of the observed and computed bending moments of the pile at G1. Both results agree well. The largest bending moment in case 2 occurred near the pile cap as in case 1. The observed bending moment for case 2 was twice that for case 1.

We can recognize that the superstructure and pile moved in opposite directions to each other in case 1 from the time histories of the accelerations (A3) and bending moments (G1). This implies that the inertia force of the superstructure decreased the amplitude of the bending moment in the piles in case 1. On the other hand, the inertial force of the superstructure increased the bending moment of the piles in case 2, because the superstructure and the piles moved in the same direction.

The power spectrum shown in Figure 11 indicates that the amplitude of the power spectrum for case 2 was smaller than that for case 1, while the maximum amplitude of the bending moment for case 2 was larger than that for case 1. Considering the results in Figure 11, the improved soil seems to be a viable means to protect piles from soil liquefaction hazard. The power spectra rather than the peak value may be a better measurement to judge the degree of criticality of damage.

## RELATIONSHIP BETWEEN COMPUTED BENDING MOMENTS AND THE AXIAL FORCE OF THE PILE WITH IMPROVED DEPOSIT

We now study the relationship between bending moments and natural frequencies of structures for case 2, by the present numerical method.

Figure 12 shows the relationship between the maximum accelerations of the structure and the maximum bending moments for natural frequencies of 12·5, 50 and 100 Hz of the superstructure in case 2. These frequencies for the prototype model correspond to 0·5, 2 and 4 Hz for the real structure, according to the similitude requirements shown in Table I. The figure indicates that larger accelerations were generated for higher natural frequencies of the structure. Thus, the responses of structures are large if they stand on stiff foundations such as a structural system of piles and improved soil, in which the input motion is not reduced when it is transmitted to the foundation basement. In contrast, the bending moment of the pile for 50 Hz was larger than those for both 12·5 and 100 Hz.

Figure 13 shows the time histories of the observed axial strain in the pile heads at G1 and G9. The vibration phase of the axial strain at G1 was opposite to that of G2 from the start of shaking in both cases. This indicates that the rocking vibration occurs in the piles–foundation system. The maximum axial strains of 110 and $300 \times 10^{-6}$ were obtained for cases 1 and 2, respectively. For case 1, however, the response of the

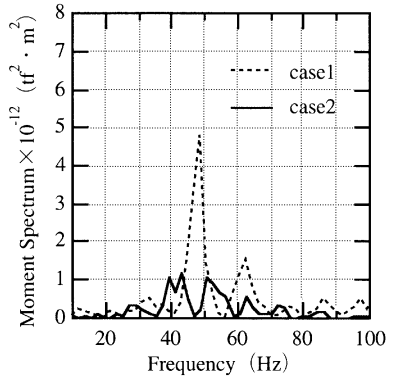


Figure 11. Comparison of the power spectrum of the bending moment of the pile at G1 for cases 1 and 2

 

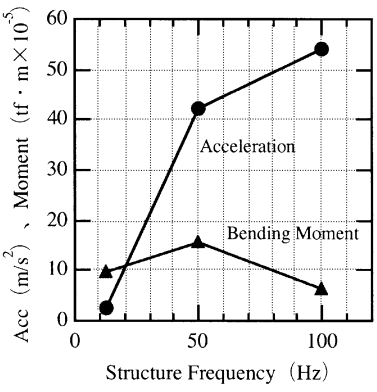


Figure 12. Relationship between maximum accelerations at A3 and bending moment at G1 under natural frequencies of 12·5, 50 and 100 Hz for the superstructure of case 2

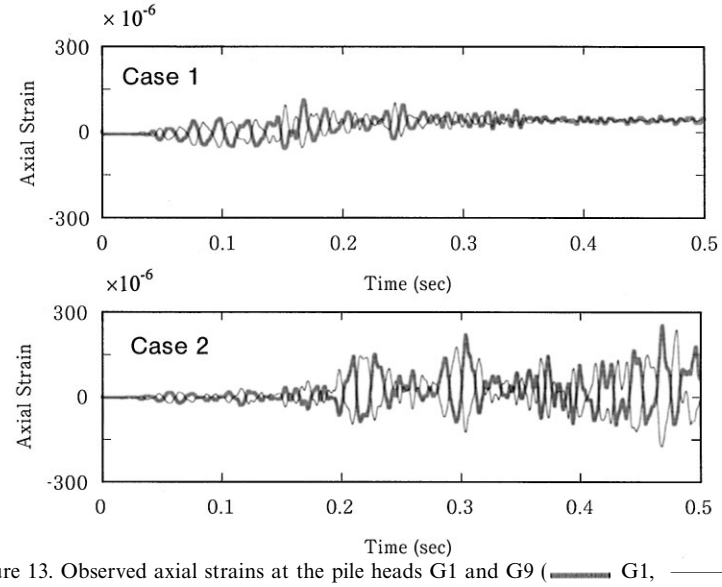


Figure 13. Observed axial strains at the pile heads G1 and G9 (▬▬ G1, ——— G9)

piles–foundation system was prominent with the transitional mode compared with the rocking mode. For case 2, the rocking vibration was predominant because the improved deposit was massive and the horizontal springs from soil to foundation became weak under liquefaction. This phenomenon depends on the size of improved deposit, the stiffness ratio of the improved deposit and the surrounding deposit, the number of piles and the pile-to-pile distance.

Figure 14 shows the relationship between the moment and the axial stress of the pile in the remedial deposit. A smaller bending moment associates with a larger axial force in the pile. This is due to the rocking vibration of the superstructure consisting of the end-bending piles and the improved deposit. Both the axial stress and the bending moment of piles should be considered in estimating the seismic capacity of the grouped pile–foundation in improved soil deposits, even if the aspect ratio of the height-to-width of the superstructure is small.

 

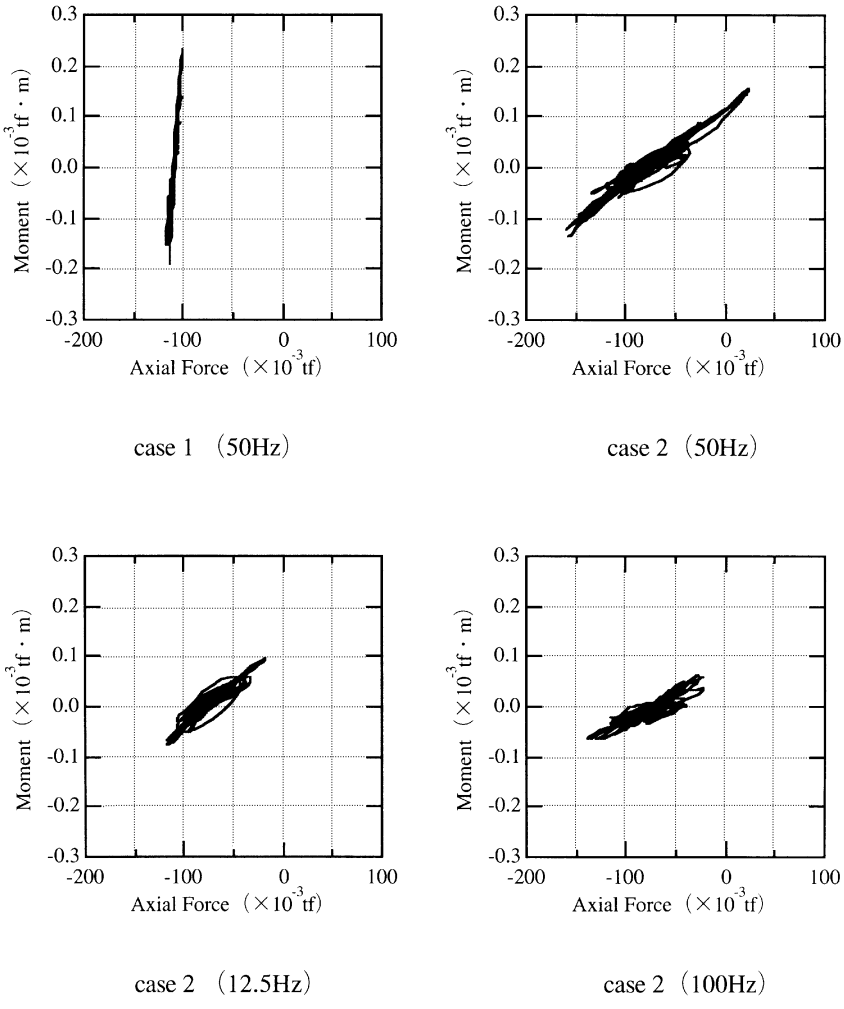


Figure 14. Relationship between the moment and the axial stress of the pile in the remedial deposit: Comparison of both responses under natural frequencies of 12·5, 50 and 100 Hz of the superstructure

## CONCLUSIONS

By comparing the results of the centrifuge tests and those of the three-dimensional effective-stress analysis, the following conclusions are obtained.

(1) The proposed analytical method proved effective. It can represent adequately the response of piles and the soil deposit under excess pore water-pressure ratios ranging from 0 to about 0·9.

(2) Significant bending moments are generated in piles in the unimproved deposits.

(3) The bending moment of the pile top in the improved deposit is about 50 per cent lower than that of the piles in the unimproved deposit. However, as a smaller bending moment is associated with larger axial stress, rocking of the structure is the dominant deformation mode of the structural system with the end-bearing piles in improved soil. The relationship between bending and axial forces is frequency dependent. It is important to consider both forces in seismic design.

 

(4) Partial ground remediation can be a viable means of protecting piles from damage due to soil liquefaction.

## REFERENCES


1. T. Nogami, J. Otani and H. L.Chen, 'Nonlinear soil pile interaction model for dynamic lateral motion', *J. Geotech. Engng. ASCE* **118**, 89–106 (1992).
2. A. Trochanis, 'A three dimensional nonlinear study of piles leading to the development of a simplified model', Ph.D. Thesis, Carnegie Mellon University, Pittsburgh, PA, 1988.
3. D. Badoni and N. Makris, 'Nonlinear response of single piles under lateral, inertial and seismic loads', *Soil Dyn. Earthquake Engng.* **15**, 29–43 (1996).
4. T. Tazoh and K. Shimizu, 'Nonlinear seismic behavior of pile foundation systems', *Proc. 10th World Conf. on Earthquake Engineering*, 1992, pp. 1807–1810.
5. T. Kagawa and L. M. Kraft, 'Lateral pile response during earthquake', *J. Geotech. Engng. ASCE* **107**, 1713–1731 (1981).
6. K.Tokimatsu and S. Nomura, 'Effects of ground deformation on pile stresses during soil liquefaction', *J. Struct. Construct. Engng. AIJ* **426**, 107–113 (1991).
7. Y. Miyamoto, K. Miura, R. F. Scott and B. Hushmand, 'Pile foundation response in liquefiable soil deposit during strong earthquakes; centrifuge test for pile foundation model and correlation analysis', *J. Struct. Construct. Engng. AIJ* **439**, 49–63 (1992).
8. W. D. Zienkiewicz and T. Shiomi, 'Dynamic behavior of saturated porous media; the generalized Biot formulation and its numerical solution', *J. Numer. Anal. Methods Geomech.* **8**, 71–96 (1984).
9. J. H. Prevost, 'Wave propagation in fluid-saturated porous media; an efficient finite element procedure', *Soil Dyn. Earthquake Engng.* **4**, 183–202 (1985).
10. M. Biot, 'Theory of propagation of elastic waves in a fluid saturated porous soil', *J. Acostic. Soc. Amer.* **28**, 168–191 (1956).
11. W. D. L. Finn, K. W. Lee and G. R. Martin, 'An effective stress model for liquefaction', *J. Geotech. Engng. Div. ASCE* **103**, 517–533 (1977).
12. W. D. L. Finn, 'Dynamic effective stress response of soil structures; theory and centrifuge model studies', *Proc. 5th Int. Conf. on Numerical Methods in Geomechanics*, 1985, pp. 35–46.
13. A. Ohtsuki and T. Itoh, 'Two-dimensional effective stress analysis of liquefaction of irregular ground including soil–structure interaction', *Earthquake Engng. Struct. Dyn.* **15**, 345–366 (1987).
14. K. Fukutake, A. Ohtsuki, M. Sato and Y. Shamoto, 'Analysis of saturated dense sand–structure system and comparison with results from shaking table test', *Earthquake Engng. Struct. Dyn.* **19**, 977–992 (1990).
15. A. Ohtsuki, M. Hirota, K. Ishimura, K. Yokoyama and K. Fukutake, 'Verification of two dimensional nonlinear analysis of sand–structure system by examining results from shaking table test', *Earthquake Engng. Struct. Dyn.* **495**, 101–110 (1993).
16. A. Ohtsuki, K. Fukutake, S. Fujikawa and M. Sato, 'Three dimensional effective analysis for evaluating response of group pile foundation under liquefaction', *Proc. Japan Soc. Civil Engrs* **495**, 101–110 (1994) (in Japanese).
17. J. O. Hallqueist, 'Theoretical manual for dyna3D', Lawrence Livermore National Laboratory, 1983.
18. F. Tatuoka and S. Fukushima, 'Stress–strain relation of sand for irregular cyclic excitation', *Seiken-Kenkyu,* Tokyo University **9**, 356–359 (1978).
19. K. Fukutake and H. Matsuoka, 'A unified law for dilatancy under multi-directional simple shearing', *Proc. Japan Soc. Civil Engrs* **412**, 143–151 (1989).
20. K. Fukutake and H. Matsuoka, 'Stress–strain relationship under multi-directional cyclic simple shearing', *Proc. Japan Soc. Civil Engrs* **463**, 75–84 (1993).
21. K. Fukutake and A. Ohtsuki, 'Prediction of preventing liquefaction of improved soil by three-dimensional analysis', *Int. Conf. on Geotechnical Engineering for Coastal Development* (GEO-COAST '91), vol. 1, 1991, pp. 447–452.
22. A. N. Schofild, 'Centrifuge test', *Soil Dyn. Earthquake engng.* **2**, 183–187 (1983).
23. R. F. Scott, 'Centrifuge model testing at Caltech', *Soil Dyn. Earthquake Engng.* **2**, 185–198 (1983).
24. J. H. Prevost and R. H. Scanlan, 'Dynamic soil–structure interaction: centrifugal modeling', *Soil Dyn. Earthquake Engng.* **2**, 212–221 (1983).
25. M. Sato, 'A new dynamic geotechnical centrifuge and performance of shaking table tests', *Proc. Int. Conf. Centrifuge 94*, Singapore, 1994, pp. 157–162.
26. M. Sato, 'Soil–pile–structure liquefaction on centrifuge', *Proc. 3rd Int. Conf. on Recent Advances in Geotechnical Earthquake Engineering and Soil Dynamics*, St. Louis, 1995, pp. 135–142.


 